Eliashberg analysis of optical spectra reveals a strong coupling of charge carriers to spin fluctuations in doped iron-pnictide $BaFe_2As_2$ superconductors

D. Wu, N. Barišić, and M. Dressel
1. Physikalisches Institut, Universität Stuttgart, Pfaffenwaldring 57, 70550 Stuttgart, Germany

G. H. Cao and Z-A. Xu
Department of Physics, Zhejiang University, Hangzhou 310027, People's Republic of China

E. Schachinger
Institute of Theoretical and Computational Physics, Graz University of Technology, 8010 Graz, Austria

J. P. Carbotte
Department of Physics and Astronomy, McMaster University, Hamilton, Ontario, Canada L8S 4M1
(Received 28 June 2010; revised manuscript received 23 September 2010; published 19 October 2010)

The temperature and frequency dependences of the optical conductivity of Co-doped $BaFe_2As_2$ are analyzed and the electron-boson spectral density $\alpha^2F(\omega)$ are extracted using Eliashberg's formalism. For the normal state at $T=30$ K there is a relatively sharp and large peak around 10 meV and a secondary smaller and broader peak centered around 50 meV with the spectrum extending to high energies beyond the maximum phonon energy. The electron-boson mass enhancement parameter is 4.4, a value more consistent with spin-fluctuation scattering rather than with phonons. In addition the spectrum is found to evolve with temperature toward a less structured background at higher energies as in the spin susceptibility.

DOI: 10.1103/PhysRevB.82.144519 PACS number(s): 74.25.Gz, 74.20.Mn, 74.20.Rp, 74.70.Xa

I. INTRODUCTION

Whenever a new family of superconductors is discovered, among the first questions posed are about the mechanism of superconductivity.[1,2] In conventional superconductors, phonons mediate the attractive interaction of two electrons forming Cooper pairs. For heavy fermions, cuprates and some organic superconductors, magnetic Cooper-pairing mechanisms have been proposed as a candidate.[3] However, intrinsic complications have prevented general acceptance. The situation of the novel class of iron-based superconductors is comparably unsettled.[4] Nevertheless, the proximity of superconductivity and antiferromagnetism in the phase diagram,[5] the weak electron-phonon interaction,[6,7] and the resonance peak in the spin-excitation spectrum[8,9] support the hypothesis of a magnetic interaction leading to superconductivity.[10–12]

The Eliashberg spectral function $\alpha^2F(\omega)$ quantifies the boson exchange effect and is a good way to discriminate between candidate mechanisms. For half a century, current-voltage characteristics obtained by tunneling spectroscopy are utilized to provide detailed and accurate information on the phonon exchange for most conventional superconductors.[13,14] In strongly correlated systems, such as high-T_c cuprates, the inversion of optical data is commonly used to extract the bosonic excitation spectra.[15–17] The analysis and interpretation, however, is not straight forward since a certain complexity in understanding the spectral signature of bosonic modes arises from the joint mechanisms in these particular systems. In this regard, Carbotte and collaborators succeeded to modify the kernel $\alpha^2F(\omega)$ of the Eliashberg theory by introducing the nearly antiferromagnetic Fermi-liquid model where the exchanged bosons are described as antiferromagnetic spin fluctuations, and the resulting optical resonance tracked very well the temperature evolution of the spin resonance seen in neutron scattering[15] but its intensity for optimum doping vanishes at T_c so that it is the remaining background which extends to large energies beyond 300 meV which accounts for the onset of superconductivity at $T=T_c$.

In this paper, we report a detailed analysis of our normal-state optical spectra obtained on $Ba(Fe_{0.92}Co_{0.08})_2As_2$ single crystals. The inversion of the frequency-dependent optical scattering rate $\tau^{-1}(\omega)$ reveals that the coupling of charge carriers to bosonic modes has an optimum peak around 10 meV with a coupling constant $\lambda=4.4$ right above T_c. With increasing temperature, this peak becomes broader and moves to higher energies and λ decreases in magnitude. These bosonic spectral properties are consistent with a magnetic mediation mechanism in the novel iron-pnictides superconductors.

II. RESULTS AND ANALYSIS

We measured the optical reflectivity of Co-doped $BaFe_2As_2$ single crystals over a wide frequency and temperature range as described in detail by Barišić *et al.*[18] The samples are well characterized and exhibit a superconducting transition at $T_c=25$ K (Ref. 19). Via Kramers-Kronig analysis we calculate the complex conductivity $\hat{\sigma}=\sigma_1+i\sigma_2$ which is further analyzed by the extended Drude model in order to obtain the frequency-dependent optical scattering rate $1/\tau(\omega)$ and the mass enhancement $m^*(\omega)/m_b=1+\lambda(\omega)$ compared to the band-mass m_b. Results are plotted in Fig. 1 for different temperatures. In principle, optical data are encoded with information on the microscopic interaction between the charge carriers. For an electron-boson system, the Eliashberg

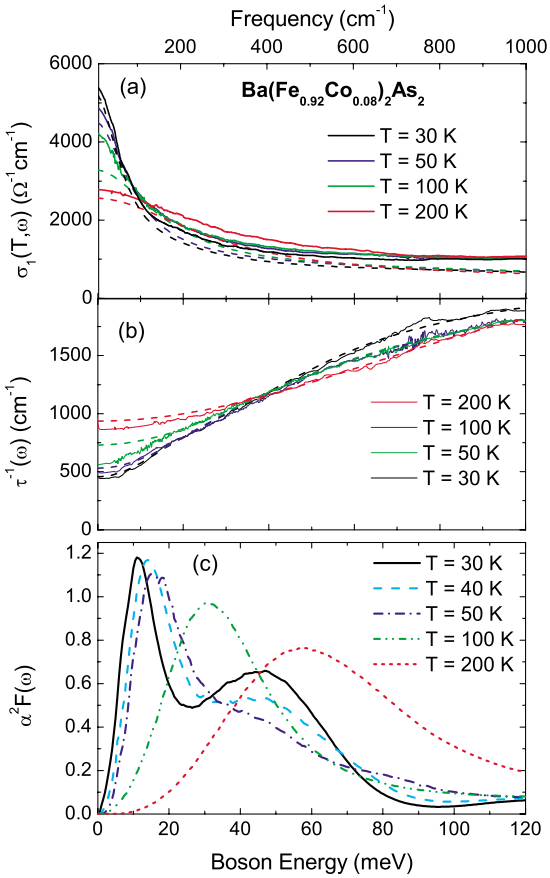

FIG. 1. (Color online) Results of the inversion calculations of the electron-boson spectral function $\alpha^2F(\omega)$ for $Ba(Fe_{0.92}Co_{0.08})_2As_2$ at different temperatures in the normal state. (a) Measured real part of the optical conductivity (solid lines) compared with computational results (dashed lines). (b) Frequency-dependent optical scattering rate obtained by the extended Drude analysis of the conductivity data plotted in panel (a) (solid lines) compared with the calculated $\tau^{-1}(\omega)$ according to Eq. (6) (dashed lines) with a constant contribution of $\tau_{\text{imp}}^{-1}=304$ cm^{-1} due to impurities. (c) The corresponding electron-boson spectral density $\alpha^2F(\omega)$ as the result of an unbiased MEM inversion.

equations apply and a Kubo formula can be used to get the infrared conductivity from the electron-boson spectral density once the quasiparticle self-energy $\Sigma(\omega,T)$ is known.[20] The opposite direction turns out to be even more challenging since we have to invert an equation of the form

$$\tau^{-1}(\omega)=\tau_{\text{imp}}^{-1}+\int_0^\infty K(\omega,\Omega;T)\alpha^2F(\Omega)d\Omega, \tag{1}$$

where τ_{imp}^{-1} denotes a constant scattering rate due to impurities. The normal-state kernel is given by[21]

$$K(\omega,\Omega;T)=\frac{\pi}{\omega}\left[2\omega\coth\left\{\frac{\hbar\Omega}{2k_BT}\right\}-(\omega-\Omega)\coth\left\{\frac{\omega+\Omega}{2k_BT/\hbar}\right\}+(\omega-\Omega)\coth\left\{\frac{\omega-\Omega}{2k_BT/\hbar}\right\}\right]. \tag{2}$$

Several methods have been suggested to extract the information on the electron-boson spectral density $\alpha^2F(\omega)$ from the optical scattering rate, such as singular value decomposition, maximum entropy method (MEM), and least-square fit; a detailed discussion of advantages and limitations of these numerical inversion techniques was given by Schachinger *et al.*[22] Here we approached the deconvolution of Eq. (1) using the MEM. We define first

$$\chi^2=\sum_{i=1}^{N}\frac{[D_i-\tau^{-1}(\omega_i)]^2}{\sigma_i^2}, \tag{3}$$

where the D_i are the data for the optical scattering rate at discrete energies ω_i. $\tau^{-1}(\omega_i)$ is defined by Eq. (1) and is a functional of $\alpha^2F(\omega)$. Finally, the σ_i are the error bars of the data and N is the number of data points D_i. Usually, χ^2 would be used in the inversion of Eq. (1) by a least-squares method minimizing χ^2 against $\alpha^2F(\omega)$. Such a straightforward approach is numerically unstable and one needs to incorporate physical constraints into the fitting process, for instance, $\alpha^2F(\omega)$ must be positive definite. To achieve this, the MEM minimizes the functional

$$L=\frac{\chi^2}{2}-aS \tag{4}$$

with χ^2 from Eq. (3) and S is the generalized Shannon-Jones entropy which gets maximized in the process. It is defined as

$$S=\int_0^\infty\left[\alpha^2F(\omega)-m(\omega)-\alpha^2F(\omega)\ln\left\{\frac{\alpha^2F(\omega)}{m(\omega)}\right\}\right]d\omega. \tag{5}$$

In Eq. (4) a is a determinative parameter that controls how close the fitting should follow the data while not violating the physical constraints. Finally, $m(\omega)$ is the constraint function (default model) which should reflect our *a priori* knowledge of $\alpha^2F(\omega)$. In an *unbiased* MEM inversion $m(\omega)=m_0$ for $\omega_1\leq\omega_i\leq\omega_N$ with m_0 some (small) constant indicating that we have no knowledge whatsoever about $\alpha^2F(\omega)$. In contrast, in a *biased* MEM inversion $m(\omega)$ is set to the Eliashberg function $\alpha^2F(\omega)$ found by other means, for instance, by unbiased inversion of another data set, maybe at some other temperature, for the same sample. Another possible choice would be to set $m(\omega)$ proportional to the measured or calculated phonon density of states if one wants to check whether or not phonons contribute dominantly to $\alpha^2F(\omega)$.

There exists a number of schemes to choose the optimal value of a in Eq. (4) based on the data and the constraint function. Here we make exclusively use of the historical method which iterates a until the average $\langle\chi^2\rangle=N$ is achieved with acceptable accuracy, i.e., the $\tau^{-1}(\omega_i)$ calculated from Eq. (1) are within σ_i of the data D_i. Nevertheless, we have to keep in mind that Eq. (2) is only an approximation to the full normal-state infinite bandwidth Eliashberg equations. Thus, in order to check the quality of the inversion it is necessary to solve these equations using the $\alpha^2F(\omega)$ of the MEM inversion in order to calculate the quasiparticle self-energy

$\Sigma(\omega,T)$. We then use a Kubo formula[20] to calculate the complex infrared conductivity $\hat{\sigma}(\omega,T)$. This finally gives the optical scattering rate via

$$\tau^{-1}(\omega,T) = \frac{\hbar\omega_p^2}{4\pi}\mathrm{Re}\left\{\frac{1}{\hat{\sigma}(\omega,T)}\right\}. \quad (6)$$

Here $\omega_p = 12\,000\ \mathrm{cm}^{-1}$ is the plasma frequency.[18] It is this so calculated scattering rate which is ultimately compared with experiment. Because of the approximate nature of Eq. (2) it is of course possible that data reproduction is not ideal and very often the $\alpha^2F(\omega)$ spectrum has to be adjusted using an additional least-squares fit procedure which is now not critical because only minor adjustments will be required.

The experimental results for the optical scattering rate $\tau^{-1}(\omega,T)$ in the metallic state of $Ba(Fe_{0.92}Co_{0.08})_2As_2$ are shown as solid lines in Fig. 1(b) for the temperatures $T=200$, 100, 50, and 30 K (from top to bottom). The inverted spectra $\alpha^2F(\omega)$ as the result of an unbiased MEM inversion are presented in Fig. 1(c). The dashed lines in Fig. 1(b) depict the results of our theoretical calculations based on the inverted $\alpha^2F(\omega)$ spectra. In this calculation we used $\tau_{\mathrm{imp}}^{-1} = 304\ \mathrm{cm}^{-1}$ to achieve the best possible agreement between experiment and theory. Before entering into a discussion of the results shown in Fig. 1 a number of additional remarks are required.

First of all, when a superconducting gap in the density of states opens below T_c, the present analysis of $\tau^{-1}(\omega)$ becomes meaningless; hence we have to restrict ourselves to $T > T_c$. However, it is safe to assume that electron-boson coupling makes a strong impact on the spectra already in the normal state just above T_c, and it is this quantity which will determine T_c. Furthermore, it is necessary to emphasize again that the Eliashberg inversion applied here is based on single-band system with infinite bandwidth while most of materials actually have finite bandwidth. The iron pnictides, on the other hand, are certainly multiband systems (see, for instance, Refs. 10 and 12). In the normal state the optical conductivity of such a multiband system is just the sum of the various band contributions to this conductivity, provided the interband optical transitions are zero or sufficiently small, as was suggested by van Heumen *et al.*[23] for the $Ba_2(Fe_{1-x}Co_x)_2As_2$ class of materials. As is generally believed, the inelastic scattering is dominated by interband transitions due to possibly spin fluctuations and, thus, a single form of the electron-boson spectral density will enter the problem except for a possible scaling factor accounting for a different magnitude of $\alpha^2F(\omega)$ for transitions between different bands. This was considered explicitly by Benfatto *et al.*[24] Thus, the application of Eq. (1) for the deconvolution of experimental data will yield meaningful information about the electron-boson interaction in such systems and will provide an *average* $\alpha^2F(\omega)$ spectrum. The shape of such a spectrum will still provide meaningful information on the bosons responsible for superconductivity, for example, phonons or spin fluctuations. Knowledge of its average magnitude is equally important. Finally, the use of a formula based on infinite bandwidth to deconvolute optical data of systems with a rather narrow bandwidth makes it extremely important to check the Kramers-Kronig consistency of $\alpha^2F(\omega)$ with optical constants to exclude any incorrect solutions due to finite bandwidth effects. Thus, in order to demonstrate the applicability of our analysis, we added the calculated $\sigma_1(\omega)$ to Fig. 1(a) as dashed lines because a good data reproduction of $\tau^{-1}(\omega,T)$ is a prerequisite of a good MEM inversion. Both cases show good agreement between theory and experiment. This gives confidence in the physical relevance of the derived spectra.

III. DISCUSSION

In Fig. 1(c), one sees a clear temperature dependence to the recovered electron-boson spectra. At temperatures just above T_c, a pronounced peak centered at 10 meV and a shoulder around 45 meV dominate the spectral weight below 80 meV. When T increases, this peak moves to higher energies and smears out quickly as does the shoulder. As a consequence, the mass renormalization factor λ is reduced from 4.4 to 1.67 at $T=200$ K. Since 10 meV seems to be a reasonable energy for phonon excitations, at first glance, it is tempting to consider a phonon mechanism for superconductivity. However, compared to band-structure calculations,[6,7] the observed spectral features are quite different. A characteristic phonon frequency ω_{ln} can be extracted; in our case $\hbar\omega_{ln} = 14.2$ meV. When the phonon mechanism is dominant in a superconducting material, one can estimate the coupling strength by its ratio to T_c. Here, we obtain $k_BT_c/\hbar\omega_{ln} = 0.15 < 0.25$, implying a conventional strong-coupling material; it also yields λ to be in the range 1–2, according to the McMillan equation.[13] Obviously, this is much too small compared to our experimental result ($\lambda = 4.4$). Here we would like to point out that the mass renormalization factor λ is widely reported to be $\lambda = 4-5$ by other studies.[25] Thus, we expect another mechanism to play the key role in mediating superconductivity in these materials. This is also very consistent with the theoretical estimate of the electron-phonon λ for the FeAs compounds which is ~ 0.2.[6] As mentioned above, spin fluctuations seem to be the natural candidate for the superconducting "glue" in iron-based materials. Whenever a magnetic mechanism is discussed, the main concern is whether spin-fluctuation exchange provides sufficient spectral intensity to make a significant impact on the electronic self-energy. Very recently, Dahm *et al.*[26] succeed to establish a quantitative relationship between the charge- and spin-excitation spectra in high-T_c cuprates, which demonstrates that the magnetic interaction can generate d-wave superconducting states with transition temperatures comparable to the maximum T_c observed in these compounds; in other words, spin fluctuations do have enough strength to cause superconducting transitions at high temperature.

In Fig. 2 we show additional results for $\alpha^2F(\omega)$ obtained from a biased MEM inversion in which the constraint function $m(\omega)$ is set to the $\alpha^2F(\omega)$ spectrum obtained from the next lower temperature. For $T=30$ K the result of the unbiased MEM inversion is presented and used as $m(\omega)$ for $T=40$ K. While there are some differences in detail with our unbiased results the trends noted in the discussion of Fig. 1(c) remain which is not necessarily always the case as has

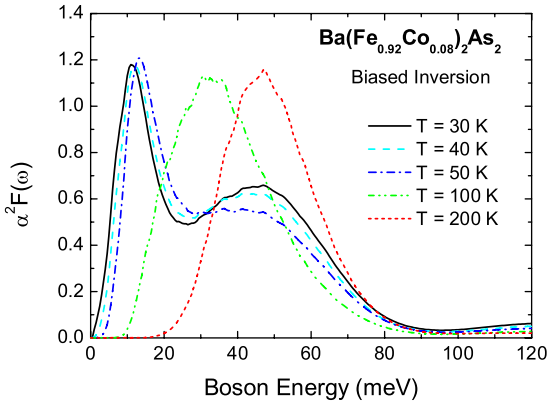

FIG. 2. (Color online) The Eliashberg function $\alpha^2F(\omega)$ for $Ba(Fe_{0.92}Co_{0.08})_2As_2$ as a function of the boson energy $\hbar\omega$ for several temperatures as a result of a biased MEM inversion.

been pointed out by Hwang *et al.*[17] While the temperature smearing is less pronounced, the movement of the peak position initially at 10 meV toward higher values and the trend toward a single peak remains. The main features are summarized in Fig. 3 where we show the mass renormalization factor λ as a function of T [solid (black) squares for unbiased and open (black) squares for biased MEM inversion, respectively] as well as the peak position as a function of T [solid (red) triangles and open (red) triangles for unbiased and biased MEM inversion, respectively]. There are only small differences in the results of the two methods of inversion and there is little ambiguity that there is a large shift in peak energy toward larger values with increasing temperature and an attendant large reduction in mass enhancement. For phonons we would expect no such changes. Our results bare also some resemblance to but differ in other aspects from inelastic polarized neutron-scattering results for the dynamic spin susceptibility $\chi''(\mathbf{Q}_{\mathrm{AFM}},\omega)$ at the antiferromagnetic wave vector $\mathbf{Q}_{\mathrm{AFM}}=\{\frac{1}{2},\frac{1}{2},1\}$. In making such a comparison

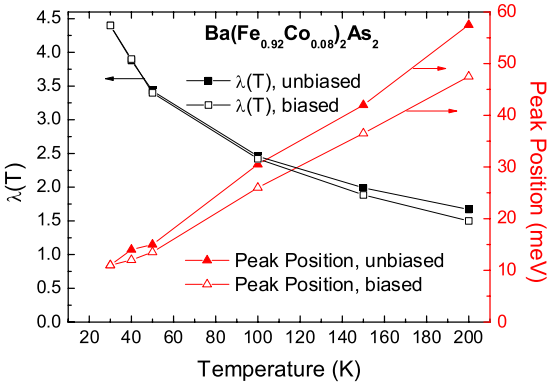

FIG. 3. (Color online) The mass enhancement factor λ(T) for $Ba(Fe_{0.92}Co_{0.08})_2As_2$ as a function of temperature T (left-hand scale applies). The solid (black) squares indicate results of an unbiased MEM inversion and the open (black) squares refer to the biased MEM inversion. Furthermore, we show the shift of the position of the main peak with temperature (right-hand scale applies). The solid (red) triangles refer to the unbiased MEM inversion while the open (red) triangles refer to the biased MEM inversion.

one needs to keep in mind that optics see an average over the spin susceptibility and not its value only at the specific momentum $\mathbf{Q}=\mathbf{Q}_{\mathrm{AFM}}$. It is the electronic transitions themselves that determine the momentum of the boson involved and in conventional metals the resulting $\alpha^2F(\omega)$ resembles closely the average phonon distribution.[27,28] Here the topology of the Fermi surfaces which are involved in the interband scattering may restrict somewhat the values of the momentum of the most important transitions but it is still expected to be an average. Nevertheless, it may differ from the local susceptibility, i.e., the average over the entire Brillouin zone as our results would indicate. The appropriate average has a peak at 10 meV at $T=T_c$ and this peaks moves to higher energies with increasing T. In the superconducting state neutron experiments the spin resonance at $\mathbf{Q}_{\mathrm{AFM}}$ is observed to move to lower energy as T increases toward T_c and its position in energy to scale roughly with temperature in accordance to the mean-field value of the temperature dependence of the BCS superconducting gap. This is different from, but not inconsistent with, our results which are limited to the normal state and deal with an average over momentum of the susceptibility rather than its $\mathbf{Q}_{\mathrm{AFM}}$-specific value, the appropriate average is determined by the interband electronic transitions themselves. It will be important to see if future spin-polarized neutron-scattering experiments can trace the origin of the 10 meV peak seen in our optical data.

Our results for $Ba(Fe_{0.95}Ni_{0.05})_2As_2$ ($T_c=20$ K) are qualitatively similar, but span only a limited energy range and exhibit excessive noise due to the smaller crystal size.[18,19] Inelastic neutron scattering indicates a resonance peak in the spin excitation spectrum around 7 meV (Ref. 9) corresponding to the lower energy scale in this material. Yang *et al.*[29] performed a similar analysis on K-doped $BaFe_2As_2$ and found two maxima of $\alpha^2F(\omega)$ in the range below 30 meV. Although different in detail, the overall accord gives us confidence that our observations reveal a general behavior in this class of materials.

IV. CONCLUSION

In conclusion, we analyzed the temperature and frequency dependences of the optical properties of Co-doped $BaFe_2As_2$ via Eliashberg theory. We obtain an electron-boson spectral density $\alpha^2F(\omega)$ which shows a strong evolution with temperature and also much larger electron-boson mass enhancement parameters [λ(30 K)=4.4 to λ(200 K)=1.6] than the electron-phonon λ=0.2. Both features indicate that, for bosonic excitations in pnictides, the spin-fluctuation scattering may play the key role rather then the phonon mechanism, as particularly the later case is expected to have a temperature-independent $\alpha^2F(\omega)$.

ACKNOWLEDGMENTS

N.B. and D.W. acknowledge support of the Alexander von Humboldt Foundation. We thank L. J. Li and X. Lin for the collaboration. J.P.C. acknowledges support by the Natural Sciences and Engineering Research Council of Canada (NSERC).

[1] S. A. Kivelson and H. Yao, Nature Mater. **7**, 927 (2008).
[2] I. I. Mazin, Nature (London) **464**, 183 (2010).
[3] *The Physics of Conventional and Unconventional Superconductors*, edited by K. H. Bennemann and J. B. Ketterson (Springer-Verlag, Berlin, 2003).
[4] K. Ishida, Y. Nakai, and H. Hosono, J. Phys. Soc. Jpn. **78**, 062001 (2009).
[5] J. W. Lynn and P. Dai, Physica C **469**, 469 (2009).
[6] L. Boeri, O. V. Dolgov, and A. A. Golubov, Phys. Rev. Lett. **101**, 026403 (2008).
[7] K.-Y. Choi, P. Lemmens, I. Eremin, G. Zwicknagl, H. Berger, G. L. Sun, D. L. Sun, and C. T. Lin, J. Phys.: Condens. Matter **22**, 115802 (2010).
[8] D. S. Inosov, J. T. Park, P. Bourges, D. L. Sun, Y. Sidis, A. Schneidewind, K. Hradil, D. Haug, C. T. Lin, B. Keimer, and V. Hinkov, Nat. Phys. **6**, 178 (2010).
[9] M. Wang, H. Luo, J. Zhao, C. Zhang, M. Wang, K. Marty, S. Chi, J. W. Lynn, A. Schneidewind, S. Li, and P. Dai, Phys. Rev. B **81**, 174524 (2010); O. J. Lipscombe, L. W. Harriger, P. G. Freeman, M. Enderle, C. Zhang, M. Wang, T. Egami, J. Hu, T. Xiang, M. R. Norman, and P. Dai, *ibid.* **82**, 064515 (2010).
[10] I. I. Mazin, D. J. Singh, M. D. Johannes, and M. H. Du, Phys. Rev. Lett. **101**, 057003 (2008).
[11] K. Kuroki, S. Onari, R. Arita, H. Usui, Y. Tanaka, H. Kontani, and H. Aoki, Phys. Rev. Lett. **101**, 087004 (2008).
[12] A. B. Vorontsov, M. G. Vavilov, and A. V. Chubukov, Phys. Rev. B **79**, 060508 (2008).
[13] J. P. Carbotte, Rev. Mod. Phys. **62**, 1027 (1990).
[14] *Superconductivity*, edited by R. D. Parks (Dekker, New York, 1969).
[15] J. P. Carbotte, E. Schachinger, and D. N. Basov, Nature (London) **401**, 354 (1999).
[16] D. N. Basov and T. Timusk, Rev. Mod. Phys. **77**, 721 (2005).
[17] J. Hwang, E. Schachinger, J. P. Carbotte, F. Gao, D. B. Tanner, and T. Timusk, Phys. Rev. Lett. **100**, 137005 (2008); J. Hwang, T. Timusk, E. Schachinger, and J. P. Carbotte, Phys. Rev. B **75**, 144508 (2007).
[18] N. Barišić, D. Wu, M. Dressel, L. J. Li, G. H. Cao, and Z. A. Xu, Phys. Rev. B **82**, 054518 (2010).
[19] D. Wu, N. Barišić, P. Kallina, A. Faridian, B. Gorshunov, N. Drichko, L. J. Li, X. Lin, G. H. Cao, Z. A. Xu, N. L. Wang, and M. Dressel, Phys. Rev. B **81**, 100512 (2010).
[20] W. Lee, D. Rainer, and W. Zimmermann, Physica C **159**, 535 (1989).
[21] S. V. Shulga, O. V. Dolgov, and E. G. Maksimov, Physica C **178**, 266 (1991).
[22] E. Schachinger, D. Neuber, and J. P. Carbotte, Phys. Rev. B **73**, 184507 (2006).
[23] E. van Heumen, Y. Huang, S. de Jong, A. B. Kuzmenko, M. S. Golden, and D. van der Marel, EPL **90**, 37005 (2010).
[24] L. Benfatto, E. Cappelluti, and C. Castellani, Phys. Rev. B **80**, 214522 (2009).
[25] D. Johnston, arXiv:1005.4392, Adv. Phys. (to be published).
[26] T. Dahm, V. Hinkov, S. V. Borisenko, A. A. Kordyuk, V. B. Zabolotnyy, J. Fink, B. Büchner, D. J. Scalapino, W. Hanke, and B. Keimer, Nat. Phys. **5**, 217 (2009).
[27] H. K. Leung, J. P. Carbotte, D. W. Taylor, and C. R. Leavens, Can. J. Phys. **54**, 1585 (1976).
[28] P. Tomlinson and J. P. Carbotte, Phys. Rev. B **13**, 4738 (1976).
[29] J. Yang, D. Hüvonen, U. Nagel, T. Rõõm, N. Ni, P. C. Canfield, S. L. Bud'ko, J. P. Carbotte, and T. Timusk, Phys. Rev. Lett. **102**, 187003 (2009).